



Electrodeposition of aluminium and aluminium/platinum alloys from AlCl_3 /benzyltrimethylammonium chloride room temperature ionic liquids

ANDREW P. ABBOTT^{1*}, CHRISTOPHER A. EARDLEY¹, NICOLA R. S. FARLEY¹, GERALD A. GRIFFITH¹ and ALLIN PRATT²

¹Chemistry Department, University of Leicester, Leicester, LE1 7RH, UK

²Johnson Matthey, Blount's Court, Sonning Common, Reading, RG4 9NH, UK

(*author for correspondence)

Received 23 July 2001; accepted in revised form 2 October 2001

Key words: alloy, aluminium, benzyltrimethylammonium, electroplating, molten salt

Abstract

This paper shows that aluminium and aluminium/platinum alloys can be deposited from room temperature ionic liquids formed from an adduct of aluminium trichloride with benzyltrimethyl ammonium chloride. The advantages of this ionic liquid over the majority of those previously investigated is that it is less water sensitive, easier to purify and form and significantly more cost effective. Voltammetry and chronoamperometry were used to investigate the deposition and stripping of aluminium on Pt, Al and Fe electrodes. Hull cell tests were performed to obtain the optimum deposition conditions and bulk electrolysis showed that uniform, adherent, crack-free aluminium deposits could be obtained from such ionic liquids. Co-electrodeposition of Al with Pt was also studied and the nucleation mechanism was found to change significantly when Pt complexes were added to the ionic solution. The platinum ligands were found to change the solubility of the complex, but had little effect on the morphology of the deposited film.

1. Introduction

The electrodeposition of aluminium has been attempted from a variety of different media. The reduction potential of aluminium precludes its deposition from aqueous solutions and studies have concentrated on using ethers [1–3], aromatic hydrocarbons [4–6] and molten salts [7–9]. Room temperature molten salts based on 1-methyl-3-ethylimidazolium chloride (MEIC) and *N*-(*n*-butyl) pyridinium chloride (BPC) with AlCl_3 form over a wide range of compositions and accordingly have marked changes in their properties. While aluminium deposition has been successfully demonstrated from both types of molten salt there are numerous difficulties associated with their use. These baths tend to be expensive, extremely water sensitive and difficult to purify and this has limited their application.

Jones and Blomgren [10] showed that a variety of other quaternary ammonium halides could be used to produce ionic liquids with AlCl_3 . They showed that trimethylphenylammonium chloride [TMPAC] produced melts with similar properties to BPC/ AlCl_3 mixtures. Aluminium deposition was demonstrated by Moy and Emmenegger et al. [11] using TMPAC/ AlCl_3 to which a small amount of a non-polar solvent had been added e.g. anisole or dichlorobenzene. Zhao and VanderNoot [12] studied aluminium electrodeposition

from pure TMPAC/ AlCl_3 but did not isolate any samples of bulk deposited metal. The area of aluminium electrodeposition from a wide range of media has recently been thoroughly reviewed [13].

In this work we describe the use of benzyltrimethylammonium chloride (BTMAC)/ AlCl_3 ionic liquids for aluminium electrodeposition and demonstrate that these have considerable advantages over other ionic liquids. It is shown that adherent, defect free aluminium can be deposited onto nickel and steel surfaces and this acts as an effective corrosion resistant coating. It is also shown that aluminium/platinum alloys can be deposited from this medium.

2. Experimental

All chemicals were handled under a dry nitrogen atmosphere in a glovebox. Aluminium chloride (Aldrich, U.K.; 99.99%) was used as received. BTMAC (Fluka, U.K.; >98%) was dried on a vacuum line at 100 °C for 24 h before use. Melts were made by slow addition of AlCl_3 to the quaternary ammonium salt in a five-necked round bottom flask and the system was continually stirred with a magnetic stirrer. The melt was heated to about 40 °C in an oil bath and then allowed to cool to ambient temperatures before measurements were

made. The melts were intensely coloured (dark brown). The colour is thought to originate from a charge transfer complex formed between the aluminium chloride and the aromatic ring on the BTMAC. If the melt constituents were not heated the melt took a lot longer to form, was a pale straw colour and had a lower conductivity than that formed by heating. Negligible difference was observed between the ^1H NMR spectra of the dark brown and the straw coloured melts. These pale coloured melts were also more susceptible to decomposition from the addition of water. Tetraamineplatinum (II) hydrogen carbonate [TPHC], and Bis(acetylacetonato) platinum (IV) [Pt(acac) $_2$] were used as received (Johnson Matthey, U.K.). Benzyltrimethylammonium hexachloroplatinate (IV) [(BTMA) $_2$ PtCl $_6$] and tetraethylammonium hexachloroplatinate (IV) [(BTMA) $_2$ PtCl $_6$] were prepared by dissolving H $_2$ PtCl $_6$ in dilute NaOH and adding an excess of the quaternary ammonium chloride to the solution. The orange precipitate thus formed was washed, filtered, recrystallised using acetone and dried under vacuum.

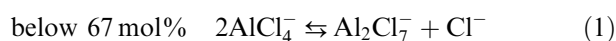
Cyclic voltammetry and chronoamperometry were carried out using a PGSTAT20 potentiostat (Ecochemie, Holland) controlled by GPES software. The working electrodes were iron, platinum or aluminium wires with a diameter of 1 mm (all Aldrich, U.K. 99.99+ %) sealed into glass and polished with alumina paste (down to 0.3 μm). The R_u of approximately 800 Ω in Figures 3 and 7 has not been compensated, but should have a negligible effect on the voltammograms. Electrodes were held at +0.6 V vs Al/Al $^{3+}$ for 30 s prior to each experiment to ensure that there was no aluminium or oxide film on the electrode surface. The counter electrode was a Pt flag of surface area 1 cm 2 . All electrochemical measurements were made at ambient temperature (21–24 $^\circ\text{C}$). All potentials are quoted with respect to an aluminium wire reference electrode which was inserted into the ionic liquid (note the reference potential will change slightly with melts of different compositions). Electrodeposition was carried out on Ni foil electrodes, which were abraded with P700 glass paper, dipped in aqua regia for 1 min, rinsed with deionised water, followed by dichloromethane and then rigorously dried before use. Post-electrolysis treatment was critical. Excess melt was removed from the sample by washing in deoxygenated toluene for 30 min. When the sample was removed from the glove box it was immediately washed with copious amounts of acetone and then dried. The morphology of the deposited films was investigated using scanning electron microscopy (SEM) and the elemental composition of these films was simultaneously determined using energy dispersive analysis by X-rays (EDAX). Conductivities of the melts were measured using a Solex model 4070 conductivity meter. All measurements were carried out at room temperature unless otherwise stated.

NMR spectra were recorded on a Bruker DRX 400 spectrometer using a 10 mm bore multiple nuclei (VSP) probe-head at 300 K. Temperature was controlled using

the standard Bruker BVT3000 temperature control accessory. ^{27}Al NMR spectra were recorded using a basic frequency of 104.26138 MHz and a 90 $^\circ$ acquire pulse (17 μs) without proton decoupling. Spectra were externally zero referenced to Al(ClO $_4$) $_3$ in H $_2$ O to produce [Al(H $_2$ O) $_6$] $^{3+}$. All samples were prepared in 5 mm NMR tubes and run coaxially inside a 10 mm NMR tube containing D $_2$ O for the lock. No corrections for susceptibility were made. Data were typically acquired using a sweep width of 26 881 Hz (257 ppm) and 32K data points, producing an acquisition time of 0.6 s and with relaxation delay of 0.4 s (total acquisition time 1 s) and 512 transients. Data was processed using an exponential multiplication of 2.5 Hz.

3. Results

Mixtures of AlCl $_3$ /BTMAC were found to be liquid at room temperature when the AlCl $_3$ composition was between 55 and 75 mol%. It was found that the advantages of using BTMAC over TMPAC were that melts using the former are easier to form (i.e. did not decompose when the AlCl $_3$ was added too rapidly) and are less susceptible to hydrolysis with water. We have recently shown that the addition of water up to 0.5 mol kg $^{-1}$ has little effect upon the electrochemical response of these media [14]. Numerous groups have studied the equilibria between the aluminium containing species in BPC and MEIC melts using NMR, EMF and transport number measurements [15–17]. These studies have shown that the principle equilibria in acidic melts are:



and

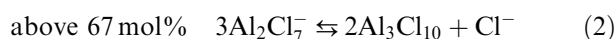


Figure 1 shows the ^{27}Al NMR spectra for AlCl $_3$ /BTMAC with mole ratios of 2:1, 1.7:1 and 1.5:1. The signal is made up of two components; that at higher field strength is due to AlCl $_4^-$ and that at lower values due to Al $_2$ Cl $_7^-$. Figure 1 shows that at 40 $^\circ\text{C}$ the equilibrium for Equation (1) lies to the right but tends to the left for less Lewis acidic compositions. The same change is observed at 25 and 60 $^\circ\text{C}$ although as the temperature is increased the equilibrium is shifted to the left and AlCl $_4^-$ is the favoured species. This is in accordance with previous results showing that the aluminium species in BTMAC melts are principally the same as BPC and MEIC melts. This is an important and surprising result as it shows that the cation has little effect on the ionic equilibria and hence the nature of the charged species in the liquid. In Table 1 the chemical shifts and line widths for the deconvoluted data shown in Figure 1 are listed. The chemical shifts for the 1.5:1 and 1.7:1 mixtures are similar whereas the 2:1 is shifted. This is probably due to

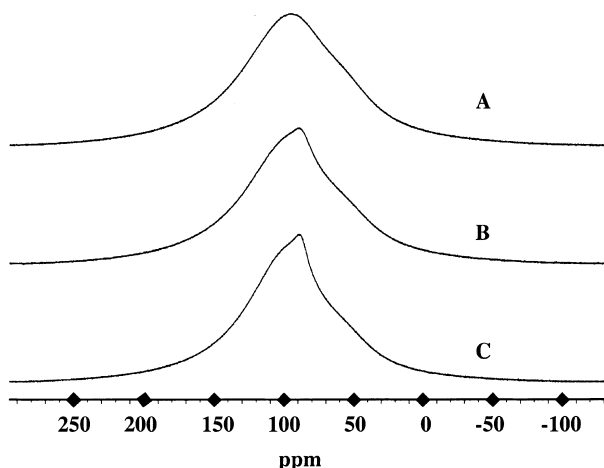


Fig. 1. ^{27}Al NMR spectra of $\text{AlCl}_3/\text{BTMAC}$ melts with mole ratios of (A) 1.5, (B) 1.7, and (C) 2:1 at 40 °C.

Table 1. Chemical shift and line width data from the deconvolution of the spectra shown in Figure 1

$\text{AlCl}_3/\text{BTMAC}$	AlCl_4^-		AlCl_2^-	
	Position/ ppm	Line width/ ppm	Position/ ppm	Line width/ ppm
1.5	115.9	61.3	98.4	22.7
1.7	117.9	60.2	98.0	23.4
2.0	136.4	51.3	107.6	51.3

the change in Al concentration in the melt. The line width for the signals also remains relatively constant for the 1.5:1 and 1.7:1 mixtures but is different for the 2:1 melt. The change in line width could be due to a change in viscosity, chemical environment or chemical exchange within the melt and it is the latter of these, which is the most likely under these circumstances. The line width values are similar to those published previously [18] although the low field strength and experimental conditions of this earlier study has led to a loss of some of the information shown in Figure 1.

Figure 2 shows the conductivity of various $\text{AlCl}_3/\text{BTMAC}$ melts as a function of temperature. The change in temperature has two effects upon the conductivity; firstly as the temperature increases the viscosity of the liquid decreases and hence the mobility of the ions increase; secondly temperature effects the position of the equilibrium in Equations (1) and (2) and the smaller ions will have a larger mobility. The conductivity of the melt increases as it becomes more Lewis acidic, which suggests that Cl^- is the major charge carrying species. The specific conductivity of these melts is similar to that of the AlCl_3/BPC melts of similar composition showing that the viscosities of the two systems are similar. It is advantageous to work in more acidic melts as the conductivity is higher and previous studies have shown that the deposition is not possible from Lewis basic melts [13]. To improve the conductivity of this ionic liquid a number of electrolytes were added. Both lithium

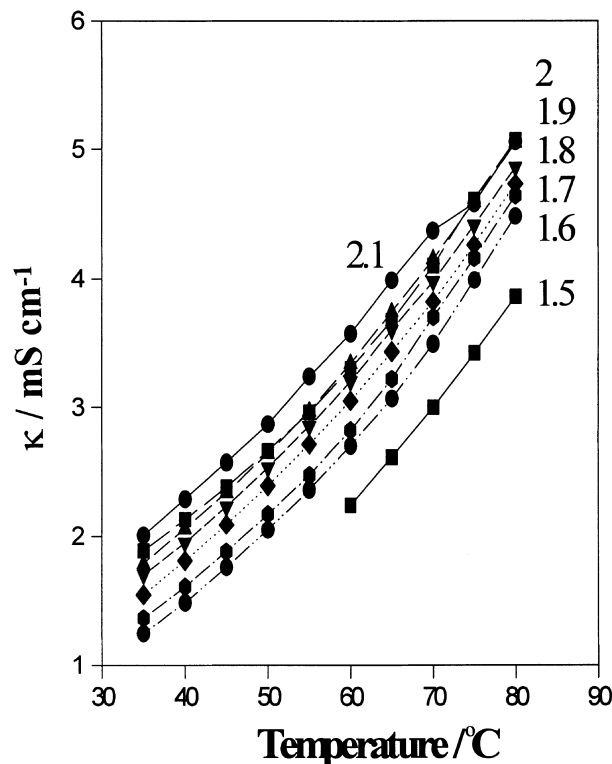


Fig. 2. Conductivity of $\text{AlCl}_3/\text{BTMAC}$ melts with various mole ratios as a function of temperature.

chloride and tetrabutylammonium tetrafluoroborate were found to be sparingly soluble in a 2:1 $\text{AlCl}_3/\text{BTMAC}$ melt and saturated solutions of both had little effect on the conductivity. BTMA BF_4 was considerably more soluble and the addition of 0.02 mol kg^{-1} to a 2:1 $\text{AlCl}_3/\text{BTMAC}$ melt caused an increase in specific conductivity from 1.48 to 1.84 mS cm^{-1} at room temperature.

Figure 3 shows the cyclic voltammogram of Fe, Al and Pt electrodes in $\text{AlCl}_3/\text{BTMAC}$ melts with mole ratios of 2:1. Results on a Ni electrode were similar to those for Pt. Iron was used primarily as an electrode material because of the importance of electrodeposition corrosion resistant coatings on steel. On an Fe electrode some evidence for underpotential deposition is observed

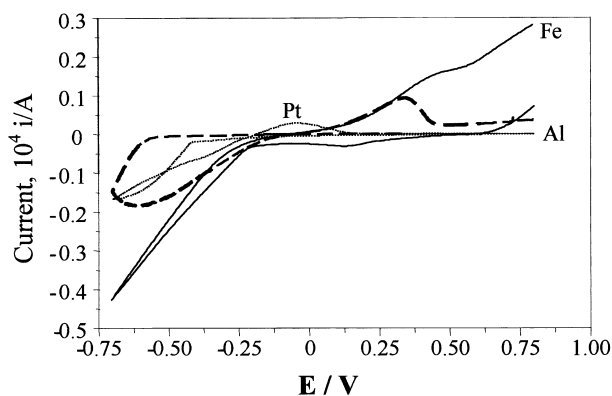


Fig. 3. Cyclic voltammetry of a 2:1 $\text{AlCl}_3/\text{BTMAC}$ melts on different electrodes. Fe (—), Al (---) and Pt (···) (sweep rate: 0.05 V s^{-1}).

at +0.2 V but this is not evident on Al or Pt. The overpotential of Al^{3+} reduction increases on different electrode materials in the order $\text{Fe} < \text{Pt} < \text{Al}$. For Al and Pt a nucleation loop was observed suggesting that on these surfaces the rate of the deposition process may be nucleation controlled. It was previously shown [14] that on an Fe electrode the reductive charge was similar to the oxidative charge irrespective of the negative sweep limit down to a potential of -0.7 V. This was, however, not the case for Pt and Al, where the charge for Al dissolution was significantly less than that for Al deposition, suggesting that the mechanism for deposition was different on these substrates. This is presumably because of the difference between the crystal structures of the deposit and the substrate.

Both the reductive and oxidative currents increased as the melt became more acidic. The reduction current at -0.6 V increased by 3-fold when the AlCl_3 :BTMAC composition of the melt changed from 1.5:1 to 2:1. Zhao and VanderNoot [12] studied the mechanism of nucleation of Al on W in straw coloured $\text{TMPAC}/\text{AlCl}_3$ melts and found that following an induction period of 0.1–0.2 s instantaneous three-dimensional nucleation occurred. This work did, however, step the potential from 0 V where it was already shown that under-potential deposition occurred and hence the results were probably for the nucleation of Al on Al where the observed rapid nucleation would be expected. Figure 4 shows a series of chronoamperometry transients at steps to -0.55 V from 0.6 V for AlCl_3 :BTMAC melts of different compositions. What is immediately noticeable from these results is a very long induction time prior to the onset of nucleation. The delay period is shorter for the less Lewis acidic melts but still considerably longer than that observed by Zhao and VanderNoot. In less Lewis acidic melts there is a larger proportion of AlCl_4^- which is easier to reduce than Al_2Cl_7^- . Figure 4 also shows that instantaneous nucleation is observed, with a negligible induction period, on Fe when the potential is stepped from 0 to -0.55 V. This suggests that under-potential deposition occurs at 0 V and the nucleation of Al on a

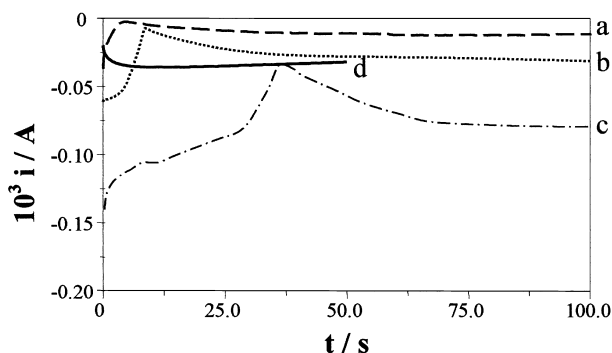


Fig. 4. Chronoamperometry of AlCl_3 /BTMAC melts with mole ratios of (a) 1.5:1 (---), (b) 1.7:1 (···), and (c) 2.0:1 (—) on an Fe electrode following a potential step from +0.6 to -0.55 V. (d) The step from 0.0 to -0.55 V for a 2:1 melt (—).

UPD layer is easier and faster than on Fe. Instantaneous nucleation was also observed on stepping from +0.6 V to -0.4 V on an Al electrode (not shown) confirming these ideas.

More negative over-potentials (≈ -0.2 V) were required to observe nucleation for the $\text{BTMAC}/\text{AlCl}_3$ than the $\text{TMPAC}/\text{AlCl}_3$ melts. Rather than being an effect of the cation, this is probably a result of the charge transfer complex formed in the former, which stabilises the aluminium species thus making it slightly more difficult to reduce. When the straw coloured $\text{BTMAC}/\text{AlCl}_3$ melt was used under-potential deposition was observed on an Al electrode confirming the above ideas.

Hull cell tests showed that the brightest and most uniform aluminium deposits were obtained at a current density was $5.1 \times 10^{-5} \text{ A cm}^{-2}$. A constant current was applied to a 1 cm^2 Ni flag electrode. At the end of a 2-h electrolysis experiment a uniform, dull, adherent deposit was observed on the electrode surface. Figure 5 shows an SEM image of the deposit formed. EDAX analysis showed that it was primarily aluminium with a trace of residual chloride. No defects or cracking of the coating layer were observed in what appeared to be an amorphous deposit. (The white, slightly cracked deposit to the left of the figure is a residue left from the ionic liquid.) To test the corrosion resistance of these coatings a Ni electrode was coated with approximately $3 \mu\text{m}$ of aluminium in a constant potential experiment (thickness estimated from charge passed). Following post-electrolysis treatment the electrode was put into an aqueous solution containing $0.1 \text{ mol dm}^{-3} \text{ KNO}_3$. Figure 6 shows a cyclic voltammogram of the electrode prior to and after coating with the aluminium layer. As can clearly be seen, no signal for nickel dissolution was observed once the aluminium layer had been deposited showing that the coating was practically defect free. The process was repeated on mild steel but a very poorly adherent, patchy, deposit was obtained which offered negligible corrosion protection.

The production of Pt/Al alloys is of great interest for the aerospace industry as these are used as coatings



Fig. 5. SEM image of a Ni electrode following a 2 h electrolysis in a 2:1 AlCl_3 :BTMAC at a constant current density of $5.1 \times 10^{-5} \text{ A cm}^{-2}$.

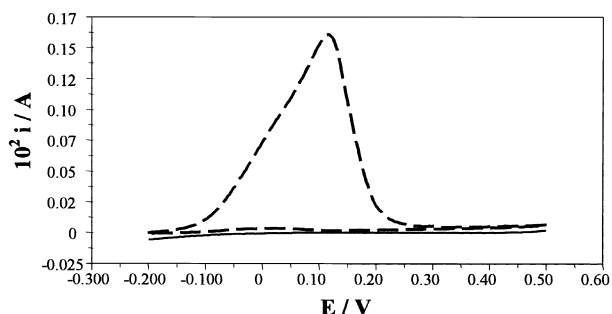


Fig. 6. Cyclic voltammogram of a Ni electrode in an aqueous solution of $0.1 \text{ mol dm}^{-3} \text{ KNO}_3$ before (---) and after (—) the deposition of Al on the surface.

for high temperature and high stress components in jet engines. The dissolution of Pt in the melt was attempted using various complexes. High solubilities ($>0.03 \text{ mol kg}^{-1}$) were achieved with tetraethylammonium and BTMA salts of $[\text{PtCl}_6]^{2-}$. Figure 7 shows the cyclic voltammogram of an Fe electrode in a 2:1 AlCl_3 :BTMAC ionic liquid prior to and following the addition of $0.03 \text{ mol kg}^{-1} \text{ BTMA}_2 \text{ PtCl}_6$. A reduction process is observed at approximately 0.1 V upon the addition of the Pt complex to the melt. The difference between the reduction potentials for platinum and aluminium in the ionic liquid is considerably lower than that expected from the standard redox potentials for Pt^{2+} and Al^{3+} , but this is a feature of ionic liquids because of the chloroaluminate and chloroplatinate complexes formed. Similar differences have also been observed for nickel and silver ions in an AlCl_3 /MEIC ionic liquid of the same composition [19, 20]. Two oxidative processes were also observed corresponding to the oxidation of the Al and Pt/Al alloy. The potentials were again similar to those observed for Ni^{2+} in an AlCl_3 /MEIC ionic liquid. Chronoamperometric experiments showed that the addition of $[\text{PtCl}_6]^{2-}$ to the ionic liquid decreased both the over-potential and time required before nucleation was observed.

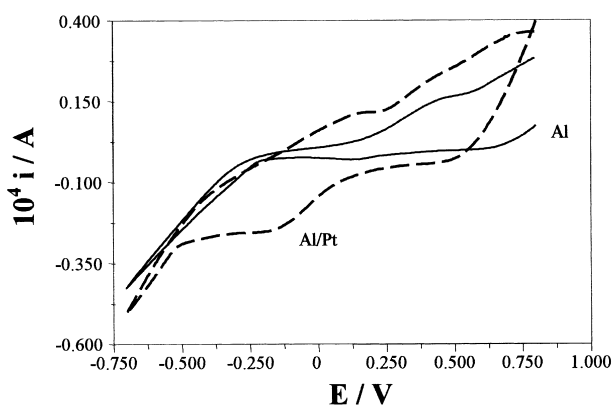


Fig. 7. Cyclic voltammogram of an Fe electrode in a 2:1 AlCl_3 :BTMAC ionic liquid prior to (—) and following (---) the addition of $0.03 \text{ mol kg}^{-1} \text{ BTMA}_2 \text{ PtCl}_6$. Sweep rate: 0.05 V s^{-1} .



Fig. 8. SEM image of a Ni electrode following a 2 h electrolysis in a 2:1 AlCl_3 :BTMAC liquid containing $0.03 \text{ mol kg}^{-1} \text{ BTMA}_2 \text{ PtCl}_6$ at a constant potential of -0.6 V .

Constant potential deposition experiments were carried out using $(\text{TEA})_2 \text{ PtCl}_6$, TPHC and $\text{Pt}(\text{acac})_2$ complexes to study the morphology and composition of the deposit as a function of the applied potential. At -1 V black, powdery, poorly adherent deposits were obtained with each of the Pt complexes, which was primarily aluminium. The chlorine content of these films was relatively high, presumably originating from chloride ions trapped in the deposit.

At -0.6 V a bright, adherent deposit was produced for all of the complexes. The platinum content of the deposits depended upon the solubility of each platinum complex in the ionic liquid. With TPHC ($0.025 \text{ mol dm}^{-3}$) an alloy containing 13% Pt was obtained, whereas with $\text{Pt}(\text{acac})_2$ where the solubility was lower (0.01 mol dm^{-3}), the Pt content was about 5% by weight. The remainder of the deposit was primarily Al while the chlorine content of all the films deposited at -0.6 V was negligible. For all of the Pt complexes studied a dense, nodular morphology was obtained for the alloyed deposit. The SEM image of a representative sample is shown in Figure 8. EDAX analysis suggested that the alloys were homogeneous. Separate layers of the two metals could, however be prepared by stepping the potential. At an applied potential of -0.2 V a bright, adherent layer of Pt was very slowly deposited. Stepping the electrode potential to -0.6 V allowed a layer of almost pure aluminium to be deposited on top of the platinum.

4. Conclusion

Aluminium and aluminium/platinum alloys can be deposited from room temperature ionic liquids based on BTMAC. The deposits are generally uniform, adherent and pinhole-free making them suitable as corrosion prevention coatings.

References

1. D.E. Couch and A. Brenner, *J. Electrochem. Soc.* **99** (1952) 234.
2. F.J. Schmidt and I.J. Hess, *Plating* **53** (1966) 229.
3. N. Ishibashi and M. Yoshio, *Electrochim. Acta* **17** (1972) 1343.
4. K. Ziegler and H. Lehmkuhl, *Angew. Chem.* **67** (1955) 424.
5. E. Peled and E. Gileadi, *Plating* **62** (1975) 342.
6. E. Peled and E. Gileadi, *J. Electrochem. Soc.* **123** (1976) 15.
7. F.H. Hurley and T.P. Wier, *J. Electrochem. Soc.* **98** (1951) 203.
8. R.A. Osteryoung and J. Robinson, *J. Am. Chem. Soc.* **102** (1980) 4415.
9. H.L. Chum and R.A. Osteryoung, In *Ionic Liquids*, D. Inman and D.G. Lovering (ed.), Plenum, New York, 1981.
10. S.D. Jones and G.E. Blomgren, *J. Electrochem. Soc.* **136** (1989) 424.
11. R. Moy and F.P. Emmenegger, *Electrochim. Acta* **37** (1992) 1061.
12. Y. Zhao and T.J. VanderNoot, *Electrochim. Acta* **42** (1997) 1639.
13. Y. Zhao and T.J. VanderNoot, *Electrochim. Acta* **42** (1997) 3.
14. A.P. Abbott, C.A. Eardley, N.R.S. Farley and A. Pratt, *Trans. Inst. Metal Finish.* **77** (1999) 26.
15. J.S. Wilkes, J.S. Frye and G.F. Reynolds, *Inorg. Chem.* **22** (1983) 3870.
16. L. Heerman and W. D'Olieslager, *Inorg. Chem.* **24** (1985) 4704.
17. R.J. Gale and R.A. Osteryoung, *Inorg. Chem.* **18** (1979) 1603.
18. J.L. Gray and G.E. Maciel, *J. Am. Chem. Soc.* **103** (1981) 7147.
19. W.R. Pitner, C.L. Hussey and G.R. Stafford, *J. Electrochem. Soc.* **143** (1996) 130.
20. C.A. Zell, F. Endres and W. Freyland, *Phys. Chem. Chem. Phys.* **1** (1999) 697.